

Effect of 1-Hexene Comonomer on Polyethylene Particle Growth and Copolymer Chemical Composition Distribution

MADRI SMIT,^{1,2} XUEJING ZHENG,^{1,2} ROBERT BRÜLL,³ JOACHIM LOOS,^{1,2} JOHN C. CHADWICK,^{1,2} COR E. KONING^{1,2}

¹Department of Chemical Engineering and Chemistry, Eindhoven University of Technology, P.O. Box 513, 5600 MB Eindhoven, The Netherlands

²Dutch Polymer Institute, P.O. Box 902, 5600 AX Eindhoven, The Netherlands

³Deutsches Kunststoff-Institut, Schlossgartenstrasse 6, 64289 Darmstadt, Germany

Received 14 November 2005; accepted 10 February 2006

DOI: 10.1002/pola.21399

Published online in Wiley InterScience (www.interscience.wiley.com).

ABSTRACT: An investigation of the polymer particle growth characteristics and polymer molecular weight and composition distributions in ethylene homopolymerization and ethylene/1-hexene copolymerization has been carried out with a catalyst comprising a zirconocene and methylaluminoxane immobilized on a silica support. The presence of 1-hexene leads to higher productivity and easier fragmentation of the support during particle growth. Crystallization analysis fractionation and gel permeation chromatography analysis of ethylene/1-hexene copolymers prepared at different polymerization times reveals a broadening of the chemical composition distribution with increasing polymerization time as a result of the gradual formation of a relatively high-molecular-weight, ethylene-rich fraction. The results are indicative of significant monomer diffusion effects in both homopolymerization and copolymerization. © 2006 Wiley Periodicals, Inc. *J Polym Sci Part A: Polym Chem* 44: 2883–2890, 2006

Keywords: copolymer chemical composition distribution; copolymerization; filter effect; metallocene catalysts; methylaluminoxane; particle growth; polyolefins; supports

INTRODUCTION

The copolymerization of ethylene with higher α -olefins has commercial importance in the production of elastomers and linear low-density polyethylene (LLDPE). Ziegler–Natta catalysts still occupy a dominant position in LLDPE manufacturing, but they suffer the disadvantage that the

comonomer distribution in the polymer is non-random as a result of the presence of different active species having different ethylene/ α -olefin reactivity ratios. The general tendency of these catalysts is to incorporate the comonomer mainly into the low-molecular-weight chains. The preferred catalysts for LLDPE are those that have a relatively uniform active center distribution, and for this reason, there has been a growing increase in the use of metallocene and related single-center catalysts, which give copolymers with narrow molecular weight and chemical composition distributions.^{1–5}

Correspondence to: J. C. Chadwick (E-mail: j.c.chadwick@polymers.nl)

Journal of Polymer Science: Part A: Polymer Chemistry, Vol. 44, 2883–2890 (2006)
© 2006 Wiley Periodicals, Inc.

The presence of higher α -olefins in ethylene polymerizations carried out with heterogeneous catalysts frequently leads to significant increases in the catalyst activity, as observed for both Ziegler–Natta^{6–14} and immobilized single-center systems.^{15–19} Various explanations for this effect have been proposed, including active site modification⁶ and an increase in the number of active centers,⁷ but there is strong evidence that a major factor in the comonomer activation effect is easier monomer diffusion, which also leads to easier particle fragmentation. A monomer diffusion limitation occurs when the monomer reactivity in polymerization is high with respect to diffusivity through the catalyst particle. This is often the case in ethylene homopolymerization when a highly crystalline polymer forms around the catalyst particle directly after the initiation of polymerization. The monomer diffuses very slowly through this crystalline mass up to a stage at which sufficient polymer has formed inside the catalyst particle to allow particle fragmentation. The addition of a small amount of a comonomer decreases the crystallinity of the polymer envelope, thus enhancing productivity. Soga et al.⁸ demonstrated that comonomer activation occurs only in cases in which homopolymerization produces a crystalline polymer. Higher ethylene polymerization activities in the presence of a comonomer have also been observed with unsupported, homogeneous metallocene catalysts^{12,20,21} but only when the polymer formed is insoluble in the reaction medium; this indicates that a diffusion limitation arises when the active catalyst becomes encapsulated in a mass of solid polymer. Comonomer activation is less common in propylene polymerization, but Jüngling et al.²² observed a threefold increase in activity when adding a small quantity of 1-octene to propylene polymerization catalyzed by a SiO₂-supported metallocene and concluded that this was due to improved monomer mass transfer in the growing polymer particle.

Monomer mass-transfer limitations can also contribute to compositional heterogeneity in ethylene/ α -olefin copolymers. This applies not only to Ziegler–Natta systems^{9,23} but also to SiO₂-supported metallocenes, with which several groups have obtained nonuniform polymer compositions not representative of single-center catalysis.^{24–26} Radial gradients in diffusivity have been proposed to account for compositional distributions in semicrystalline ethylene/propylene copolymers,²⁴ and Fink et al.²⁵ ascribed the compositional distribu-

tion of ethylene/1-hexene copolymers prepared with a SiO₂/methylaluminoxane (MAO)/zirconocene system to the formation, during the initial stages of polymerization, of a copolymer envelope around the catalyst particle. The easier diffusion of the smaller monomer, ethylene, with respect to 1-hexene was proposed to lead to a polymer particle comprising an ethylene-rich center surrounded by an outer layer of the copolymer, thus giving a broad overall chemical composition distribution. The term *filter effect* was coined to describe this phenomenon.

In this study, we have investigated the particle fragmentation and growth characteristics and molecular composition of ethylene homopolymers and copolymers, using a catalyst prepared by the immobilization of MAO and racemic ethylene bridged bis(indenyl) zirconium dichloride [*rac*-Et(Ind)₂ZrCl₂] on a Sylopol 948 silica support precalcined at 600 °C and having a residual OH content of 1.0 mmol/g. Gel permeation chromatography (GPC) and crystallization analysis fractionation (CRYSTAF) analysis of ethylene/1-hexene copolymers obtained at various stages of polymerization shows that the copolymer composition distribution broadens with increasing polymerization time, in line with the filter effect proposed by Fink et al.²⁵

EXPERIMENTAL

Materials

All reactions were carried out under an argon atmosphere. A 10 wt % solution of MAO in toluene was obtained from Witco, whereas *rac*-Et(Ind)₂ZrCl₂ was purchased from Strem Chemicals. The silica support material, Sylopol 948, was kindly donated by Grace AG and calcined at 600 °C before use, as described previously.²⁷ Toluene (Biosolve) was dried on alumina columns, whereas *n*-heptane was distilled over potassium before use. Triisobutylaluminum (TIBA) was purchased from Akzo–Nobel as a 25 wt % solution in toluene. Ethylene (Air Liquide) was dried over columns containing activated copper catalyst (BTS) and alumina before introduction into the polymerization reactor.

Catalyst Immobilization

Catalyst immobilization was carried out by 23.9 μ mol of *rac*-Et(Ind)₂ZrCl₂ being brought into

contact with 3.12 mmol MAO (10 wt % in toluene) for 10 min, after which the resulting solution was slowly added to 1 g of silica in 1.5 mL of toluene at 0 °C. After a further 10 min, the temperature was gradually increased under reduced pressure to 63 °C over a period of 5 h to give a free-flowing powder.

Slurry Polymerization Procedure

The polymerization was carried out in a 1-L autoclave equipped with a hollow-shaft turbine stirrer and a temperature-controlled heating/cooling mantle. *n*-Heptane (400 mL) was charged to the reactor under an argon atmosphere, and after it was heated to 50 °C, an ethylene monomer pressure of 2.4 ± 0.1 bar was applied, and the reactor contents were stirred for 30 min at 1000 rpm to ensure maximum dissolution of the gaseous monomer. TIBA (1.8 mmol) was then added (via a pressure injector system), along with the desired amount of 1-hexene and 75 mL of *n*-heptane. After 15 min, the immobilized catalyst (150 mg) was charged to the reactor with 75 mL of *n*-heptane. After 1 h of polymerization at 50 °C, the reactor was degassed, and the slurry was quenched with acidic methanol. The polymer was dried *in vacuo* at 60 °C.

Polymer Characterization

High-temperature GPC was carried out in 1,2,4-trichlorobenzene at 140 °C with a GPC PL 220 from Polymer Laboratories with refractive-index detection. A column system consisting of five polystyrene columns of the following specifications were used: PSS SDV 10^7 , 10^6 , 10^5 , 10^3 , and 100 Å. A calibration using polystyrene standards was applied.

The copolymer chemical composition distribution was measured by CRYSTAF with a model 200 from PolymerChar SA (Valencia). The sample was dissolved at 160 °C in 1,2,4-trichloroben-

zene, and the solution (concentration 0.5 mg/mL) was stabilized at 100 °C and then cooled to 20 °C at 0.1 °C/min.

Differential scanning calorimetry (DSC) was carried out with a Q100 differential scanning calorimeter (TA Instruments). The samples (1.5–2.5 mg) were heated to 160 °C at a rate of 10 °C/min and cooled at the same rate to –50 °C. A second heating cycle at 10 °C/min was used for data analysis.

Hexene comonomer contents in selected polymers were determined by ^{13}C NMR (125.69 MHz) spectroscopy with a Varian Unity Inova 500 NMR spectrometer at 120 °C in 1,2,4-trichlorobenzene with deuterated tetrachloroethane as the lock solvent.

RESULTS AND DISCUSSION

The immobilized metallocene catalyst used in this work, containing 0.17 wt % Zr and 8.6 wt % Al, was prepared by the impregnation of silica with a mixture of MAO and *rac*-Et(Ind) $_2$ ZrCl $_2$.²⁷ The silica support, Sylopol 948 (obtained from Grace), was first calcined at 600 °C, after which the residual content of the surface hydroxyl was 1.0 mmol/g and the surface area and pore volume were 304 m 2 /g and 1.8 cm 3 /g, respectively. After impregnation, the surface area was 270 m 2 /g, and the pore volume was 1.2 cm 3 /g. The MAO/zirconocene immobilization also led to a decrease in the average pore diameter, from 24 to 17 nm.

Ethylene Homopolymerization

To facilitate an investigation of the effect of the polymerization time on the catalyst/support particle fragmentation and polymer composition, ethylene polymerizations were carried out in heptane slurry at 50 °C with a relatively low monomer pressure of 2.4 bar. The results are given in Table 1. The decrease in the productiv-

Table 1. Ethylene Homopolymers

Sample	Polymerization Time (min)	Productivity (kg/mol of Zr h)	M_n (g/mol)	M_w (g/mol)	M_w/M_n	Melting Temperature (°C)
E1	6	1,700	151,900	475,900	3.1	127
E2	10	1,700	139,400	541,500	3.9	129
E3	30	800	140,700	539,700	3.8	131
E4	60	700	160,900	558,000	3.5	131
E5	300	400	144,600	496,300	3.4	131

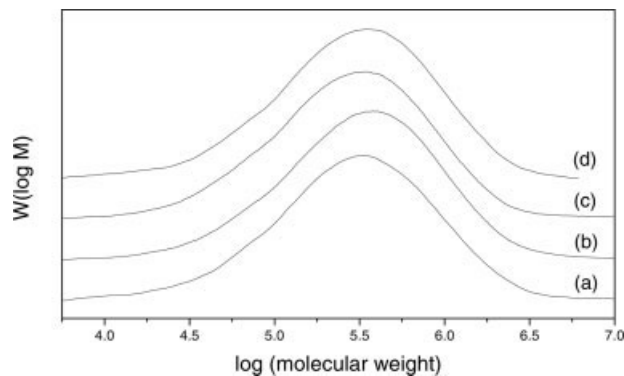


Figure 1. Molecular weight distributions of polyethylene after (a) 6, (b) 30, (c) 60, and (d) 300 min of polymerization.

ity, expressed per hour, from very short polymerization times to long polymerization times is indicative of diminishing activity throughout the course of the polymerization.

The molecular weight distributions of these ethylene homopolymers were somewhat broader than the Schulz–Flory distribution [weight-average molecular weight/number-average molecular weight (M_w/M_n) = 2], which would be consistent with ideal single-center behavior of the catalyst, although our previous results²⁷ have shown that this immobilized catalyst gives polypropylenes with the expected very narrow molecular weight distributions. The molecular weight distribu-

tions of the polyethylenes are shown in Figure 1, from which it is apparent that, regardless of the polymerization time, a unimodal distribution has been obtained.

Ray et al.²⁸ illustrated the possibility of diffusion-controlled reactions and broadening of molecular weight distributions, as a result of large concentration gradients in the growing polymer particle, in their work on the multigrain model of particle growth. To check whether this phenomenon could explain the somewhat broader molecular weight distribution of the polyethylenes, compared with that of polypropylene, the particle morphology and fragmentation behavior were studied.

Scanning electron microscopy (SEM) micrographs of the particle morphologies of polyethylenes obtained after 6, 60, and 300 min of polymerization are shown in Figure 2. The formation of stretched fibrils on the particle surface is evident at a high magnification [Fig. 2(d–f)] and is typically indicative of a diffusion-controlled particle growth mechanism. The formation of a polymer layer around a yet unfragmented core of the catalyst/support particle is clearly evident from cross-sectional SEM imaging of a particle obtained after 6 min of polymerization, as shown in Figure 3(a). Distinct polymer and silica phases can even be observed after 60 min of polymerization [Fig. 3(b)], whereas after 300 min of polymerization [Fig. 3(c)], complete fragmen-

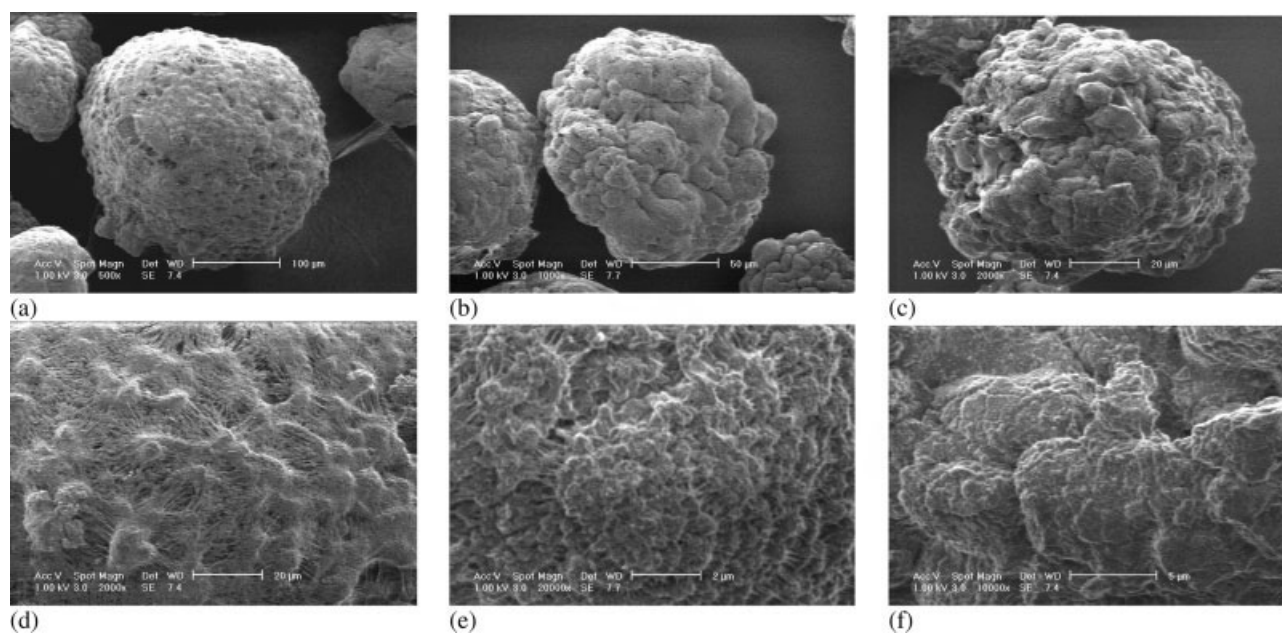


Figure 2. Particle morphology of polyethylenes obtained after (a,d) 6, (b,e) 60, and (c,f) 300 min of polymerization.

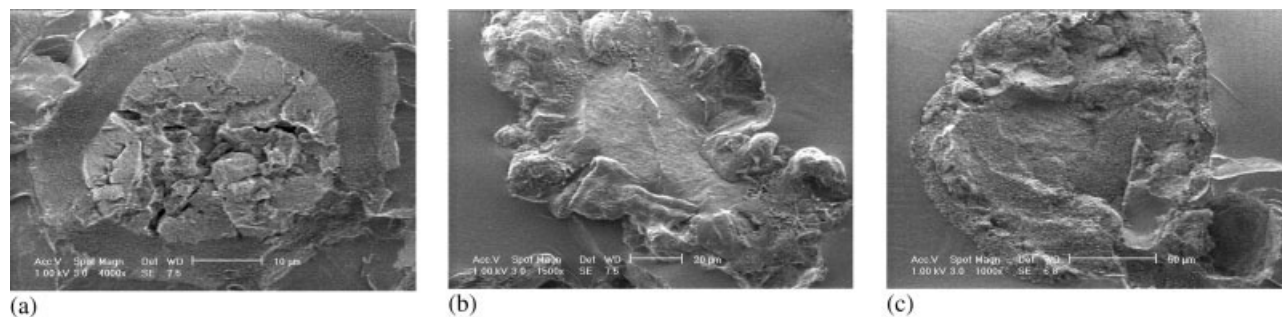


Figure 3. SEM cross-sectional imaging of polyethylene particles obtained after (a) 6, (b) 60, and (c) 300 min of polymerization.

tation of the support appears to have taken place.

Ethylene/1-Hexene Copolymerization

The effect of the introduction of a comonomer on the ethylene polymerization activity and polymer particle growth, as well as on the compositional uniformity of the resulting copolymer, was investigated in a series of polymerizations in which the ethylene pressure was kept constant at 2.4 bar and the 1-hexene concentration was varied between 0.05 and 0.35 mol/L. As in the case of ethylene homopolymerization, polymerization times of 6, 30, 60, and 300 min were selected. The polymerization results are shown in Table 2, from which it can be seen that with a very short polymerization time (6 min), the productivity increased with increasing 1-hexene concentration. For 60 min of polymerization, the highest productivity was observed with a 1-

hexene concentration of 0.09 mol/L; further increases in the comonomer concentration led to lower activity, as reported for other systems.^{10,18,29}

The molecular weights of the various copolymers in Table 2 are significantly lower than those of the corresponding ethylene homopolymers in Table 1. This is characteristic of metallocene-based catalyst systems;^{29,30} the comonomer promotes chain termination. The molecular weight distributions are still broader than would be expected for a single-center catalyst, and for the polymers prepared at relatively low 1-hexene concentrations, a consistent broadening of the molecular weight distribution with increasing polymerization time is apparent. The changes in the molecular weight distribution with the polymerization time are shown in Figure 4. The appearance of a shoulder at a high molecular weight is apparent, and this is consistent with a mechanism in which a high-molecular-

Table 2. Ethylene/1-Hexene Copolymers

Sample	1-Hexene in the Polymerization (mol/L)	Hexene in the Copolymer (mol %)	Time (min)	Productivity (kg/mol of Zr h)	M_n (g/mol)	M_w (g/mol)	M_w/M_n	Melting Temperature (°C)
EH1	0.05		6	800	86,600	223,400	2.6	112
EH2	0.05		30	700	89,000	270,800	3.0	120
EH3	0.05	1.8	60	800	69,300	313,600	4.5	120
EH4	0.05		300	700	66,800	316,500	4.7	123
EH5	0.09		6	900	74,200	193,800	2.6	103 (118)
EH6	0.09		30	700	76,100	230,900	3.0	119 (100)
EH7	0.09	3.1	60	1,400	85,100	303,700	3.6	97 (117)
EH8	0.09		300	800	— ^a	— ^a	— ^a	121 (97)
EH9	0.17		6	1,000	81,400	349,300	4.3	83 (123)
EH11	0.17	5.2	60	600	86,500	326,600	3.8	85 (121)
EH12	0.35		6	3,600	— ^a	— ^a	— ^a	80 (123)
EH13	0.35	8.4	60	400	76,800	296,700	3.9	124 (84)

^a Not determined.

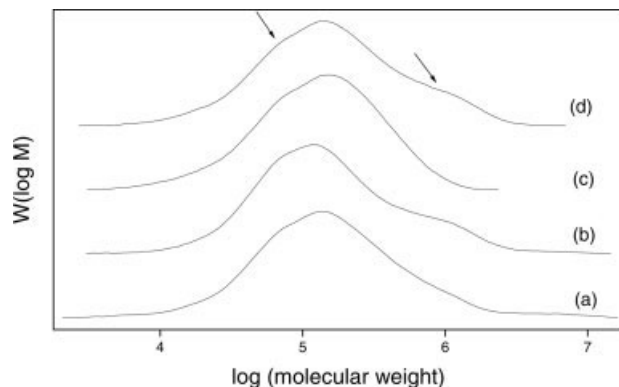


Figure 4. Molecular weight distributions of (a,b) copolymers obtained after 6 and 60 min, respectively, at [1-hexene] = 0.09 mol/L and (c,d) copolymers obtained after 6 and 60 min, respectively, at [1-hexene] = 0.17 mol/L.

weight, ethylene-rich fraction forms in the particle interior as a result of easier diffusion of ethylene in comparison with 1-hexene.

To determine the effects of the polymerization time in more detail, the resulting copolymers were analyzed with CRYSTAF. This fractionation technique, introduced into polymer analysis in the 1990s, makes use of the fact that the temperature at which an ethylene/ α -olefin copolymer crystallizes from solution varies according to the comonomer content.³¹ The CRYSTAF profile is therefore dependent on the chemical composition distribution of the polymer.

The CRYSTAF profiles of copolymers obtained after different polymerization times, with 1-hexene concentrations of 0.05 and 0.09 mol/L, are shown in Figure 5. A significant broadening with increasing polymerization time is apparent, indicative of a broadening of the chemical composition distribution. In the case of the copoly-

mers synthesized with the lower concentration of 1-hexene, a broad crystallization peak can be observed between 47 and 87 °C up to a polymerization time of 60 min. With longer reaction times, the crystallization profile becomes bimodal, and a pronounced peak at 82–83 °C develops. The CRYSTAF analysis of the copolymers prepared at a higher 1-hexene concentration [Fig. 5(ii)] reveals the presence of two distinct fractions even at the initial stage of polymerization (6 min). As expected, the higher 1-hexene concentration gave polymers with higher comonomer contents, as evidenced by both the relative proportions and peak crystallization temperatures of fractions present in each polymer. Relatively low comonomer contents of the fractions crystallizing around 80 °C are indicated by the fact that the peak crystallization temperature of a polyethylene homopolymer prepared under the same polymerization conditions (300 min of polymerization) was observed at 88 °C. The experimental error of the peak temperature in CRYSTAF analysis is ± 1 °C.³²

Soares and coworkers^{26,33} proposed that bimodality in the chemical composition distributions of ethylene/1-hexene copolymers prepared with supported metallocene catalysts was indicative of the existence of more than one active center. However, the polydispersity of the 0.09 mol/L 1-hexene sample after 6 min of polymerization is 2.6 and thus indicates single-center behavior. It is therefore not likely that the appearance of dual peaks in the CRYSTAF profile is due to the presence of two types of active centers in this catalyst system. The fact that we observe a change in the crystallinity distribution at various stages of polymerization and at various 1-hexene concentrations indicates that the bimodality observed in this work can be best des-

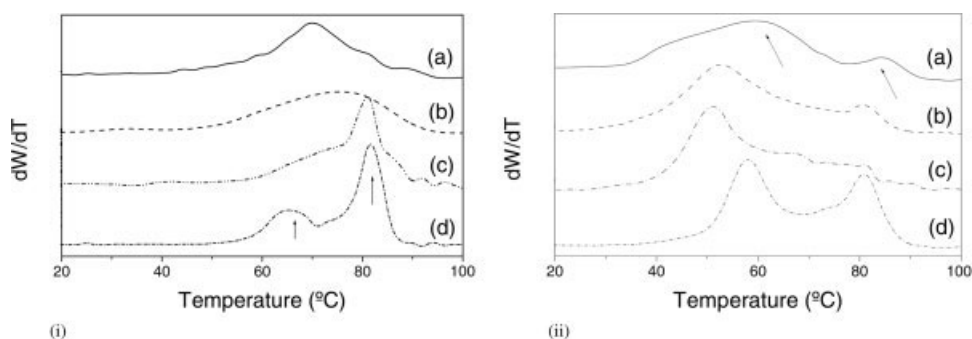


Figure 5. CRYSTAF analysis of copolymers prepared at initial 1-hexene concentrations of (i) 0.05 and (ii) 0.09 mol/L after (a) 6, (b) 30, (c) 60, and (d) 300 min of polymerization.

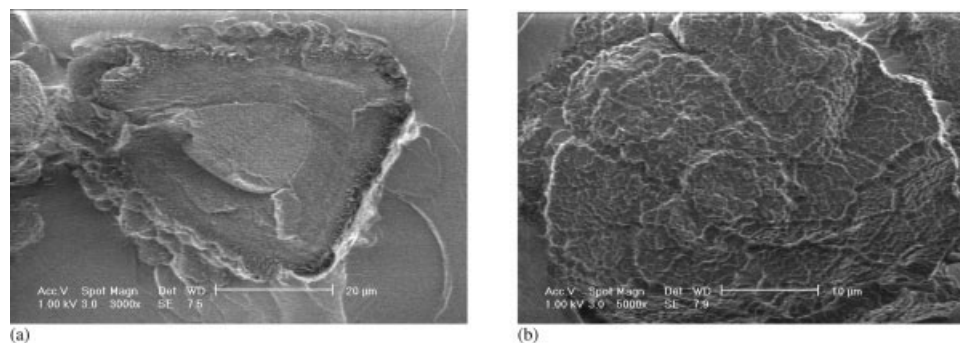


Figure 6. Particle cross-sectional images of (a) ethylene homopolymer sample E4 and (b) ethylene/1-hexene copolymer sample EH12.

cribed by the filter effect.²⁵ In these polymerizations, only around 1% of the 1-hexene present was consumed, and the results cannot be explained by significant changes in the comonomer concentration during the course of polymerization. In the initial stages of copolymerization (after 6 min), the first peak observed at the low temperature side in the CRYSTAF profiles correlates to 1-hexene-rich fractions, as best illustrated by the sample prepared at a 1-hexene concentration of 0.05 mol/L. In the filter effect theory, it is assumed that 1-hexene-rich polymer chains will form initially on the surface of the solid catalyst particle and that more rapid diffusion of the smaller ethylene monomer will subsequently result in a more polyethylene-rich core. A further factor to be taken into account is increased monomer sorption in the amorphous phase of the copolymer being formed.³⁴

The effect of comonomer incorporation on particle fragmentation during polymerization is illustrated in Figure 6. Cross-sectional SEM images of particles of an ethylene homopolymer obtained after 60 min (E4 in Table 1) and an ethylene/1-hexene copolymer obtained after only 6 min (EH12 in Table 2) are shown in Figure 6(a,b), respectively. In contrast to the incomplete fragmentation evident in the homopolymer, full fragmentation of the catalyst/support particle is obtained within a mere 6 min in the presence of a relatively high concentration of 1-hexene.

CONCLUSIONS

Diffusion limitations in ethylene homopolymerization and copolymerization with an immobilized single-center metallocene catalyst can result in a broadening of the polymer molecular

weight distribution and chemical composition distribution. Catalyst/support fragmentation during polymer particle growth is greatly accelerated by the presence of 1-hexene as a comonomer. The copolymer composition broadens with increasing polymerization time as a result of the gradual formation of an ethylene-rich fraction in addition to the main copolymer fraction. These results support Fink's filter model, in which it is proposed that the formation of an ethylene-rich fraction arises from easier diffusion of ethylene, with respect to 1-hexene, through a copolymer envelope formed in the outer regions of the catalyst particle.

This work forms part of the Research Programme of the Dutch Polymer Institute (DPI) project #111.

REFERENCES AND NOTES

- Brintzinger, H. H.; Fischer, D.; Mülhaupt, R.; Rieger, B.; Waymouth, R. M. *Angew Chem Int Ed Engl* 1995, 34, 1143–1170.
- Kaminsky, W. *J Polym Sci Part A: Polym Chem* 2004, 42, 3911–3924.
- Mülhaupt, R. *Macromol Chem Phys* 2003, 204, 289–327.
- McKnight, A. L.; Waymouth, R. M. *Chem Rev* 1998, 98, 2587–2598.
- Gabriel, C.; Lilge, D. *Polymer* 2001, 42, 297–303.
- Calabro, D. C.; Lo, F. Y. In *Transition Metal Catalyzed Polymerizations: Ziegler–Natta and Metathesis Polymerizations*; Quirk, R. P., Ed.; Cambridge University Press: Cambridge, England, 1988; pp 729–739.
- Tait, P. J. T.; Downs, G. W.; Akinbani, A. A. In *Transition Metal Catalyzed Polymerizations: Ziegler–Natta and Metathesis Polymerizations*; Quirk, R. P., Ed.; Cambridge University Press: Cambridge, England, 1988; pp 834–860.

8. Soga, K.; Yanagihara, H.; Lee, D. *Makromol Chem* 1989, 190, 995–1006.
9. Wang, J.; Zhang, W.; Huang, B. *Makromol Chem Macromol Symp* 1992, 63, 245–258.
10. Chien, J. C. W.; Nozaki, T. *J Polym Sci Part A: Polym Chem* 1993, 31, 227–237.
11. Kim, I.; Kim, J. H.; Choi, H. K.; Chung, M. C.; Woo, S. I. *J Appl Polym Sci* 1993, 48, 721–730.
12. Koivumäki, J.; Seppälä, J. V. *Macromolecules* 1993, 26, 5535–5538.
13. Pasquet, V.; Spitz, R. *Makromol Chem* 1993, 194, 451–461.
14. Wester, T. S.; Ystenes, M. *Macromol Chem Phys* 1997, 198, 1623–1648.
15. Echevskaya, L. G.; Zakharov, V. A.; Semikolevna, N. V.; Mikenas, T. B. *Polimery* 2001, 46, 40–43.
16. Bortolussi, F.; Broyer, J.-P.; Spitz, R.; Boisson, C. *Macromol Chem Phys* 2002, 203, 2501–2507.
17. Ko, Y. S.; Woo, S. I. *J Polym Sci Part A: Polym Chem* 2003, 41, 2171–2179.
18. Kumkaew, P.; Wu, L.; Praserttham, P.; Wanke, S. E. *Polymer* 2003, 44, 4791–4803.
19. Zhou, J.-M.; Li, N.-H.; Bu, N.-Y.; Lynch, D. T.; Wanke, S. E. *J Appl Polym Sci* 2003, 90, 1319–1330.
20. Tsutsui, T.; Kashiwa, N. *Polym Commun* 1988, 29, 180–183.
21. Kim, I.; Ha, C.-S. *Polym Bull* 2004, 52, 133–139.
22. Jüngling, S.; Koltzenburg, S.; Mülhaupt, R. *J Polym Sci Part A: Polym Chem* 1997, 35, 1–8.
23. Wang, J.; Pang, D.; Huang, B. *Polym Bull* 1990, 23, 127–131.
24. Hoel, E. I.; Cozewith, C.; Byrne, G. D. *AIChE J* 1994, 40, 1669–1684.
25. Przbyla, C.; Tesche, B.; Fink, G. *Macromol Rapid Commun* 1999, 20, 328–332.
26. Kim, J. D.; Soares, J. B. P. *Macromol Rapid Commun* 1999, 20, 347–350.
27. Smit, M.; Zheng, X.; Loos, J.; Chadwick, J. C.; Koning, C. E. *J Polym Sci Part A: Polym Chem* 2005, 43, 2734–2748.
28. Nagel, E. J.; Kirillov, V. A.; Ray, W. H. *Ind Eng Chem Prod Res Dev* 1980, 19, 372–379.
29. Heiland, K.; Kaminsky, W. *Makromol Chem* 1992, 193, 601–610.
30. Seppälä, J.; Koivumäki, J.; Liu, X. *J Polym Sci Part A: Polym Chem* 1993, 31, 3447–3452.
31. Monrabal, B.; Blanco, J.; Nieto, J.; Soares, J. B. P. *J Polym Sci Part A: Polym Chem* 1999, 37, 89–93.
32. Anantawaraskul, S.; Soares, J. B. P.; Wood-Adams, P. M.; Monrabal, B. *Polymer* 2003, 44, 2393–2401.
33. Chu, K.-J.; Shan, C. L. P.; Soares, J. B. P.; Penlidis, A. *Macromol Chem Phys* 1999, 200, 2372–2376.
34. Hutchinson, R. A.; Ray, W. H. *J Appl Polym Sci* 1990, 41, 51–81.